J Mater Sci (2010) 45:1955–1962
DOI 10.1007/s10853-009-4187-z

Synthesis of a fullerene/expanded graphite composite and its lubricating properties

Shoji Yoshimoto · Junji Amano · Kouji Miura

Received: 29 September 2009 / Accepted: 28 December 2009 / Published online: 14 January 2010

Abstract A fullerene/expanded graphite composite, in which fullerene crystals were incorporated into the expanded graphite interspaces, was prepared by chemical and thermal treatments and its lubricating properties in commercial grease were investigated. Expanded graphite, which was synthesized from graphite by oxidizing by $KMnO_4$ in 98% H_2SO_4 containing $NaNO_3$ and by heating at 400 °C for 3 min, and fullerene were placed in a stainless steel tube, and were heated in a furnace under vacuum at 600 °C for 2 weeks. The fullerene/expanded graphite composite obtained was characterized by X-ray diffraction analysis (XRD), Fourier transform infrared (FT-IR) spectroscopy, and scanning electron microscopy (SEM). XRD and FT-IR analyses showed that crystalline fullerene was present in the material and SEM images confirmed that it existed in the expanded graphite interspaces. The composite was blended with a commercial grease, and its lubricating properties were investigated using a four-ball lubricant tester. These properties were evaluated by measuring the wear scar diameter and wear volume loss of the test ball. The combination of composite and grease provided a better lubricating performance than that of pure graphite and grease.

S. Yoshimoto (✉)
Aichi Industrial Technology Institute, 1-157-1, Onda-cho, Kariya, Aichi 448-0013, Japan
e-mail: shoji_yoshimoto@pref.aichi.lg.jp

J. Amano
Innovation Plaza Tokai, Japan Science and Technology Agency, 23-1, Ahara-cho, Minami-ku, Nagoya 457-0063, Japan

K. Miura
Department of Physics, Aichi University of Education, Hirosawa, Igaya-cho, Kariya Aichi 448-8542, Japan

Introduction

A composite material is generally described as a combination of two or more phases at the macroscopic level, which will result in an improved system with superior characteristics than that of its individual components by themselves. Nanocomposites are a relatively new class of composites that have gained recognition in recent years, due to their unique reinforcement properties [1]. Nanocomposites composed of organic polymer and inorganic layered host are new type of composites that have been developed recently. These nanocomposites are almost obtained by intercalating polymers (or a monomer subsequently polymerized) inside the galleries of inorganic layered host and exhibit unexpected remarkable hybrid properties synergistically derived from two components [1, 2]. Graphite [3–9] and clays [10–12] are some examples of layered solids capable of intercalation.

Graphite is a layered material, consisting of a structure where carbon atoms are bonded covalently in a hexagonal arrangement within the layer and only van der Waals forces are acting between successive layers. Since the van der Waals forces are relatively weak, it is possible for a wide range of atoms, molecules, and ions to intercalate between graphite layers and that produces the graphite intercalation compounds (GICs) [13, 14]. In contrast to the clays, however, there are no reactive ion groups on the graphite layers. It is difficult to intercalate organic molecules or polymers directly into the interlayer of graphite through ion exchange reaction to prepare the polymer/graphite nanocomposites. The expanded graphite, a kind of modified graphite, contains abundant pores ranging from 10 to 100 nm. The expanded graphite has a large interlayer spacing with a layered structure as natural flake graphite [13]. Therefore, some monomers, initiators, and polymers are able to be introduced into

the pores and galleries of expanded graphite to produce polymer/graphite nanocomposites and many polymer/graphite macrocomposites have been extensively synthesized to enhance the mechanical, physical, electrical properties, and so on [3–9].

In contrast, fullerenes (C_{60}), a class of sphere-shaped molecules, were observed for the first time in 1985 [15] and isolated in bulk in 1990 [16]. Since then C_{60} has attracted a lot of attention and given rise to a very significant number of investigations. Potential applications of C_{60} include the preparation of pharmaceuticals [17–19], lubricants [20–24], and superconductors [25, 26]. Graphite is also valued in industrial applications for its self-lubricating and dry lubricating properties. It is well-known that lubricating properties of graphite are due to the loose interlamellar coupling between sheets in the structure. C_{60} intercalated graphite have previously been designed, and the electronic properties and stability have been studied theoretically [27]. It is also reported that the C_{60} intercalated graphite may possess potential applications in superconductor [28] and hydrogen storage device [29]. Fullerene molecules, especially C_{60}, also possess unique lubrication effects and they have been treated as a lubricant due to its spherical shape [30–32]. Although, it can also be expected that GICs are suitable as superlubricants, very few investigations have been devoted to the use of GICs as practical lubricants. The combination of GIC and C_{60} expects to provide synergistic effects beyond individual performance. Recently, we have shown that a C_{60} monolayer system confined by graphite walls exhibits superlubricity, ultralow spatial-average friction [33–35].

In the present study, we synthesized the composite consisting of C_{60} and expanded graphite. Synthesized C_{60}/expanded graphite composite was characterized by X-ray diffraction (XRD), Fourier transform infrared (FT-IR) spectroscopy, and scanning electron microscopy (SEM). In addition, we investigated the lubricating properties of the resulting composite using the four-ball lubricant tester and considered its possibility as the lubricating additive of the commercial grease experimentally.

Experimental

Materials

The natural graphite used for preparing the expanded graphite was purchased from Nippon Carbon Co., Ltd. It was flake graphite with an average size of 500 μm. C_{60} used in this experiment was purchased from Frontier Carbon Co., Ltd in Japan. All other reagents used such as sulfuric acid (H_2SO_4), potassium permanganate ($KMnO_4$), sodium nitrate ($NaNO_3$), and hydrogen peroxide (H_2O_2) were analytical grade.

Characterization and measurements

X-ray powder diffraction patterns were obtained on a Rigaku RINT 2200/PC diffractometer with CuKα radiation at 40 kV and 30 mA. Fourier transform infrared spectra of the samples in KBr pellets were recorded on a JASCO 480 Plus FT-IR spectrometer. The morphologies of the composites were examined using scanning electron microscopy (SEM S-3000, Hitachi) at a 15 kV accelerated voltage. The specific surface area was measured with a Mountech Macsorb HM model-1210 BET surface area analyzer. The tribological behavior of the obtained samples was investigated on the Shinko Engineering Co., Ltd. four-ball lubricant tester. The balls used in the tests are made of SUJ2 steel (composition, C: 0.95–1.10%; Si: 0.15–0.35%; Mn: <0.50%; P: <0.025%; S: <0.025%; Cr: 1.30–1.60%; Fe: balance) with a diameter of 12.7 mm (0.5 inch) and a hardness of HRC 62-65. The lubricating tests were operated by rotating the steel ball at 1,200 rpm under a 441N load for 1 h at room temperature by using the lubrication of 2 g grease containing 1% additive. The wear scar diameter (WSD) and wear volume loss were taken as a measure of the antiwear characteristics of the test composition. An optical microscope was used to determine WSD of the three lower balls with an accurate reading of 0.01 mm, then the average of the three WSDs and wear volume losses were calculated.

Preparation of expanded graphite

Expanded graphite was prepared following the procedures. As a first step, graphite oxide (GO) was synthesized from natural graphite by Hummer's method [36]. Graphite (2 g) was oxidized by $KMnO_4$ (6 g) in 98% H_2SO_4 (46 mL) containing $NaNO_3$ (1 g) at 0 °C for 0.5 h and then the mixture was stirred at room temperature for 20 h. After reacting sufficiently, 92 mL of distilled water was slowly added into the mixture and the mixture was kept for 15 min. The reaction was terminated by the addition of a large amount of distilled water (280 mL) and H_2O_2 solution (20 mL). The resulting mixture was centrifuged and washed with distilled water repeatedly to remove metal ions. The brown product undergoes dialysis for 14 days to completely remove metal ions and acids. After the dialysis, the products were subsequently dried under vacuum and GO was obtained. The expanded graphite was prepared by heating GO at 400 °C for 180 s. Hereafter, the expanded graphite prepared from GO is abbreviated as EGO.

Preparation of fullerene/expanded graphite composite material

A fullerene/expanded graphite oxide (C_{60}/EGO) composite material was prepared as follows according to the

literatures [16]. C_{60} and EGO in 2:1 weight ratio were taken in a stainless tube, and were heated in a furnace under vacuum at 600 °C for 2 weeks. The product obtained was washed by toluene lightly to remove the fullerene adsorbed on the surface, and was dried at 80 °C.

Results and discussion

Graphite is a layered compound which is characterized by strong interlayer covalent bonds of carbon atoms within each layer and weak van der Waals interaction between carbon planes. The interlayer distance of pure graphite is 3.35 Å ($2\theta = 26.6°$ for XRD measurement). It is well-known that layer lattice structure of graphite makes it possible to be intercalated by a variety of atoms and molecules, and the GICs are produced. Expanded graphite can be made from GICs through intercalated acid into the graphite interlayer. In order to introduce the acid into the interlayer, an oxidant is necessary to be used. Expanded graphite has generally been prepared by heating the expandable graphite at about 1050 °C which was treated with concentrated H_2SO_4 and HNO_3. The expanded graphite prepared from concentrated H_2SO_4 and HNO_3 is abbreviated as EG to distinguish from EGO. The XRD pattern of EG is shown in Fig. 1b, together with that of pristine flake graphite (Fig. 1a). The XRD pattern of EG still shows the sharp peak corresponding to the (002) plane of graphite at $2\theta = 26.6°$. This means that the lots of graphite layers with d-spacing of 3.35 Å remains in the EG prepared. Thus, in this study, flake graphite was converted

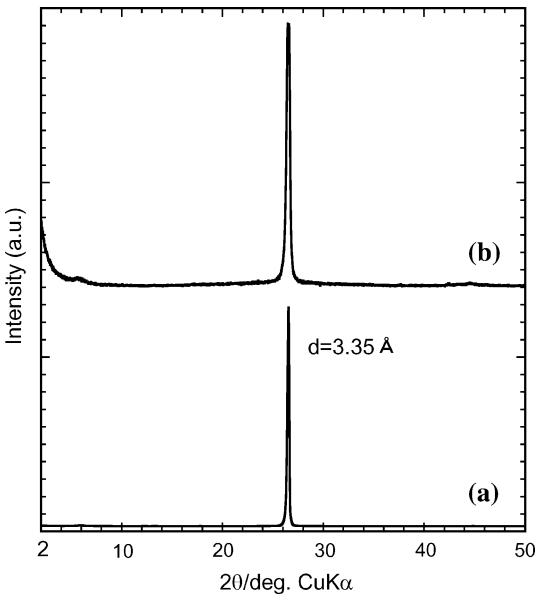

Fig. 1 X-ray diffraction patterns of *a* pure graphite and *b* EG

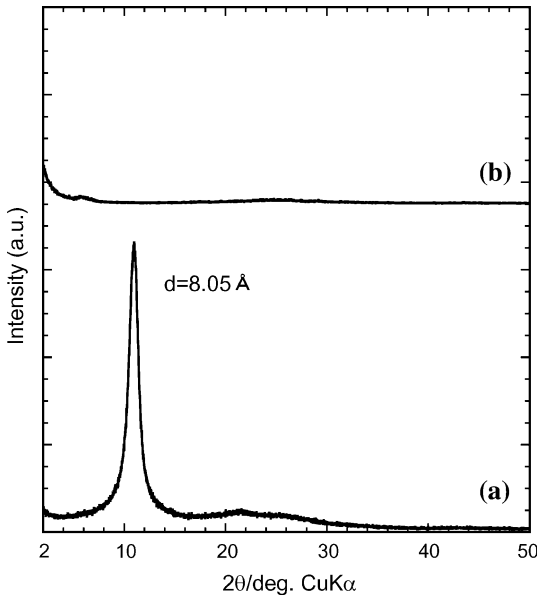

Fig. 2 X-ray diffraction patterns of *a* GO and *b* EGO

to GO by reaction with $KMnO_4$ and $NaNO_3$, followed by producing expanded graphite by heating at 400 °C for 180 s. Figure 2 shows the XRD patterns of GO and EGO. It is obvious that the diffraction peak corresponding to a layer structure of GO shifts to lower 2θ values at $2\theta = 10°$ as compared to pristine graphite, which indicates that the layers in graphite are completely oxidized and that the compound having new layer distance is produced. The XRD pattern of EGO gave no clear peak, which suggests that the stacked sheets of GO were almost entirely exfoliated by heating. The SEM micrographs of the expanded graphite prepared different methods are shown in Fig. 3. The SEM images show that the morphologies of the expanded graphite are strongly affected by the preparation methods. After expansion, the EG was a loose and vermicular morphology, while EGO was orderly and porous one. The layer distance, in other words "pores size", of EGO is approximately 100–300 nm and the thickness of the GO sheets in the EGO found by SEM is several tens of nanometer. That is, the most of layered structures of GO, in which several sheets are stacked with nanoscale thickness, were expanded by thermal treatment. The SEM images are in good agreement with the XRD results. The specific surface area by N_2 gas adsorption technique (BET) is also another popular technique for evaluating the porous materials. After measuring the specific surface area of the expanded graphite, those of EG and EGO are 10.6 and 330.4 m^2/g, respectively. The specific surface area of EGO is approximately more than 30-fold grater than that of EG and this result implies that the preparation process of EGO would progress precisely as observed for the SEM results.

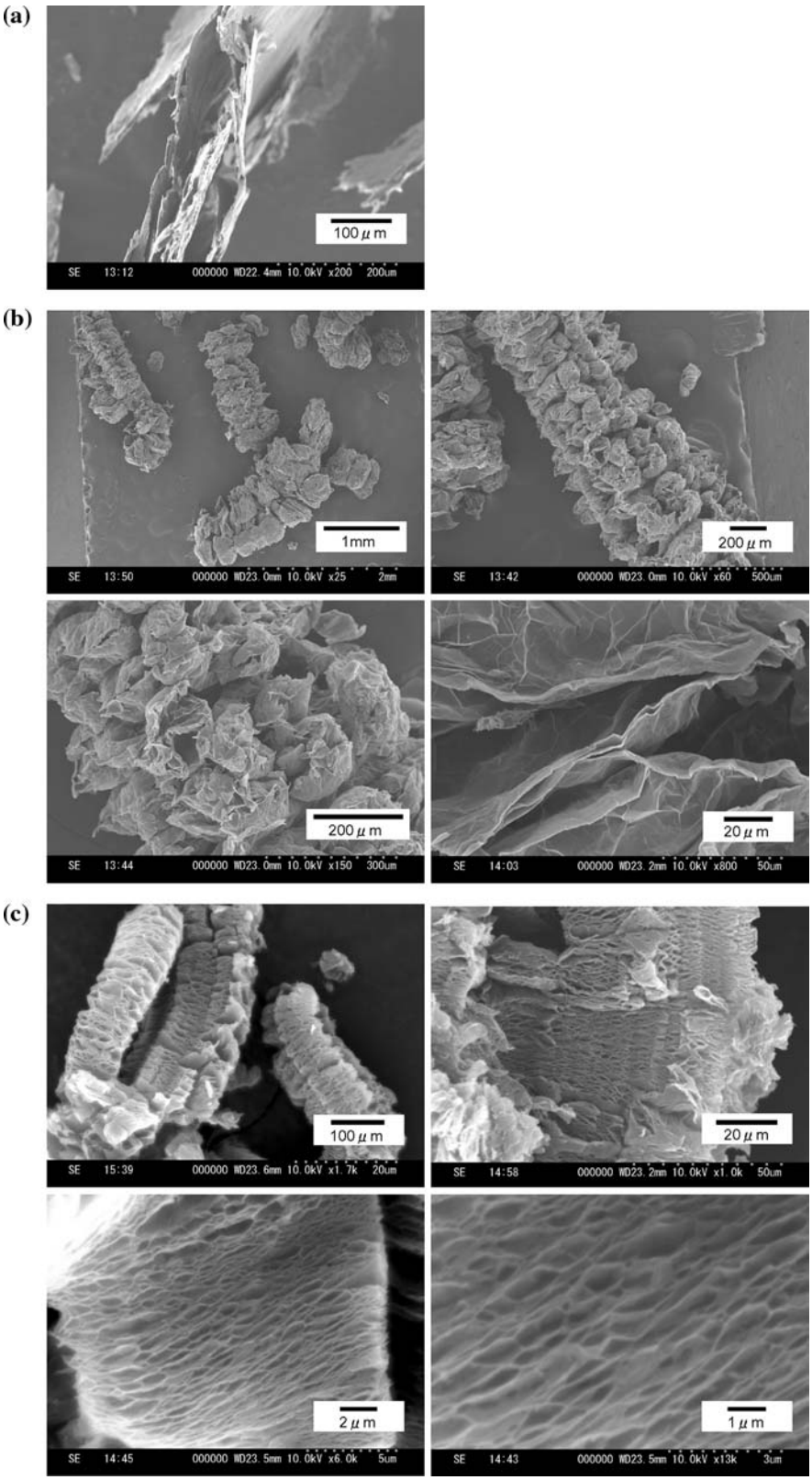

Fig. 3 SEM micrographs of **a** pure graphite, **b** EG and **c** EGO

On the basis of XRD and SEM results, the synthetic processes of the expanded graphite are proposed, and are schematically depicted in Fig. 4.

As described in experimental part, C_{60}/EGO composite was synthesized by heating the C_{60} and EGO in a stainless tube putted in a furnace under vacuum at 600 °C for

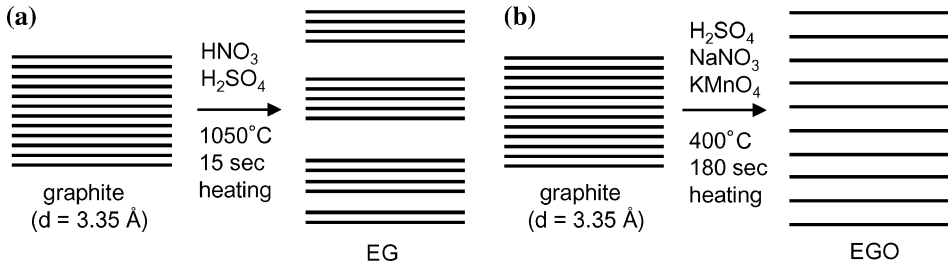

Fig. 4 Proposed schematic illustrations of the preparation process of **a** EG and **b** EGO

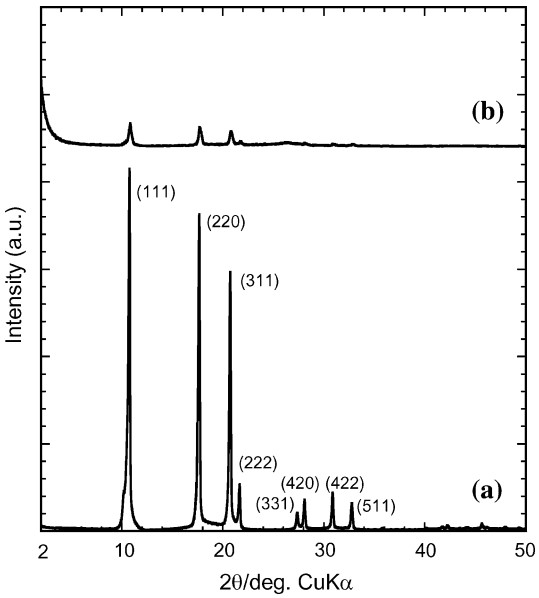

Fig. 5 X-ray diffraction patterns of *a* pure C_{60} and *b* C_{60}/EGO composite

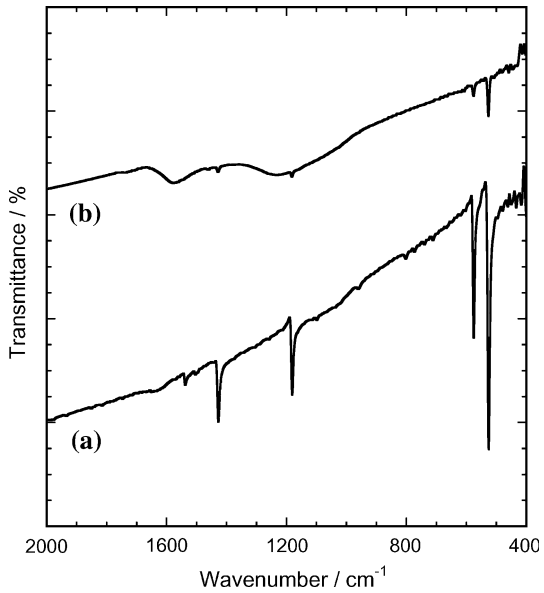

Fig. 6 FT-IR spectra of *a* pure C_{60} and *b* C_{60}/EGO composite

2 weeks. The XRD patterns of the product obtained in this way and pristine C_{60} are shown in Fig. 5. It is well-known that C_{60} adopts the face-centered cubic (fcc) close-packed structure with lattice constant $a = 14.17$ Å at room temperature [37]. In the XRD pattern of C_{60}, the characteristic peaks are attributed to the (111), (220), (311), (222), (331), (420), (422), and (511) planes, respectively (JCPDS file No.44-0558). These peaks assigned to the C_{60} were also observed in the XRD pattern of the C_{60}/EGO composite. The calculated interlayer distance that C_{60} was intercalated into the graphite interlayers has already been reported. According to the literature, the equilibrium interlayer distance is c.a. 1.3 nm in the graphite/C_{60}/graphite sandwiched system [28, 29, 35]. The XRD pattern of the C_{60}/EGO composite prepared in this study does not show the diffraction peak corresponding to 1.3 nm and some peaks attributed to the C_{60} crystal instead. This would suggest that the C_{60} exists as the crystalline state in the C_{60}/EGO composite. In other words, this shows that the C_{60}/EGO composite prepared in this study does not form the graphite/C_{60}/graphite sandwiched system.

Fourier transform infrared (FT-IR) spectra are shown in Fig. 6. Figure 6a and b shows the spectra of pure C_{60} and the C_{60}/EGO composite, respectively. The FT-IR spectrum of the C_{60}/EGO composite clearly gives the four sharp characteristic peaks of C_{60} molecule centered at 527, 576, 1183, and 1428 cm^{-1} [16].

X-ray diffraction analysis (XRD) and FT-IR analyses do not exactly show the incorporation of C_{60} into the EGO interspaces. The SEM image is expected to be the effective tool to confirm the morphology of the C_{60}/EGO composite. Figure 7 shows the SEM micrographs of the C_{60}/EGO composite and pristine C_{60}. As described above, solid C_{60} adopts fcc crystal at room temperature and the SEM image of pure C_{60} certainly seems to be crystalline morphology as can be seen in Fig. 7a. The crystalline C_{60} is observed in the images of the C_{60}/EGO composite (Fig. 7b). In Fig. 7b, the layered structure in which several sheets are stacked with nanoscale thickness represents EGO and it can be clearly observed that the crystalline C_{60} is incorporated into those interspaces. The size of crystalline C_{60} is approximately several 100 nm and the interspaces of EGO are crammed full with C_{60}. The SEM images of the C_{60}/EGO composite also indicate that excess crystalline C_{60},

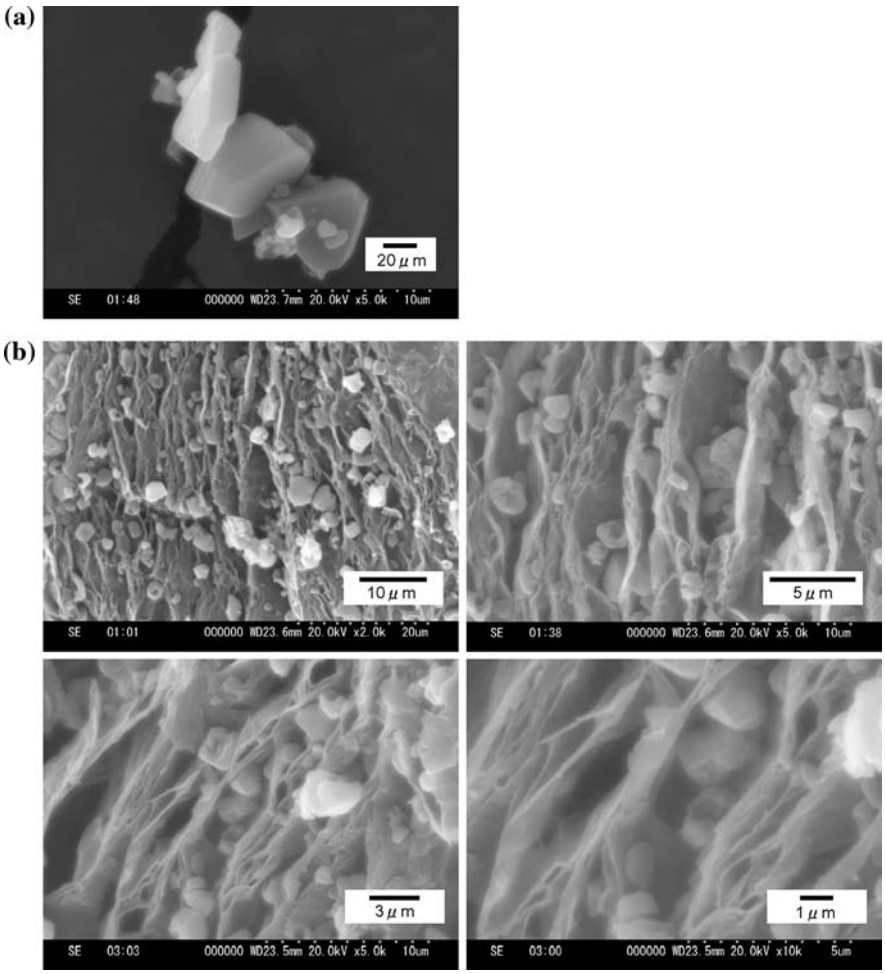

Fig. 7 SEM micrographs of **a** C_{60} and **b** C_{60}/EGO composite

which cannot be incorporated into the EGO interspaces, deposited outside the EGO layers.

Many lubricant agents contain solid particles, such as commercial colloidal dispersions of graphite, tungsten disulfide, molybdenum disulfide (MoS_2), or polytetrafluoroethylene as additive to enhance the lubricating ability of the base oil or grease. Their lubricating properties are generally attributed to a layered structure on the molecular level with weak bonding between layers. Such layers are able to slide relative to each other with minimal applied force, thus giving them their good tribological properties. We have shown thus far that a C_{60} monolayer system confined by graphite layers exhibits superlubricity, ultralow spatial-average friction by using Friction Force Microscope [33–35]. In this system, C_{60} molecules act as molecular bearings, assisted by the nanogears of six-membered carbon rings between C_{60} molecules and graphite, in which the mean dynamical frictional forces are zero up to a high load of 100 nN. In the C_{60}/EGO composite prepared in this study, the XRD and SEM results suggest that C_{60} does not form a monolayer system but forms the fcc crystal in EGO interspaces. Thus, it is expected that the C_{60}/EGO composite does not provide the same highly tribological behaviors as a C_{60} monolayer system. We added the C_{60}/EGO composite to the commercially available grease and evaluated the performance of that as the additive of lubricant. The lubricating performance is tested using a four-ball tester. The machine including the four-ball tribosystem has been used to determine the lubricant properties. The four-ball test is the industrial standard test method for measuring the wear preventive characteristics of a lubricant. Placed in a bath of the test lubricant, three fixed steel balls are put into contact with a fourth ball in rotating contact at set conditions. Lubricant wear protection properties are measured by comparing the average wear scars on the three fixed balls. The smaller the average wear scar, the better the protection. The C_{60}/EGO composite was added to the base grease and the lubricant wear protection properties of the grease were investigated. Similarly, the lubricating properties of the greases blended with widely used additives such as graphite and MoS_2 were also studied. The lubricating tests were carried out under the lubrication of 2 g grease containing 1.0% additives. Those were evaluated by measuring

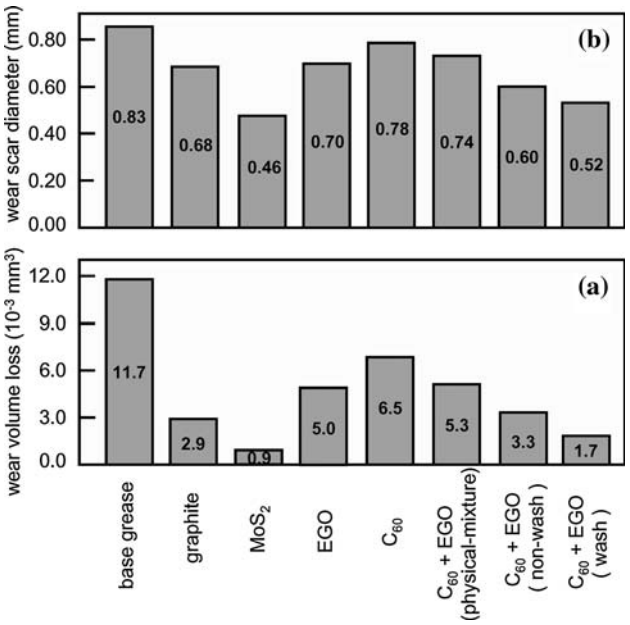

Fig. 8 Lubricating properties of the grease with various kinds of additives, **a** wear volume loss and **b** wear scar diameter

the wear scar diameter (WSD) and wear volume loss of the test ball. The test was conducted at a rotating speed of 1200 rpm and a constant load of 441N for 1 h. The results of the wear behaviors for some lubricating additives are shown in Fig. 8. According to Fig. 8, the WSD and wear volume loss of the test ball for the base grease were 0.83 mm and 11.7×10^{-3}mm^3, respectively. It can be seen that the WSD of the greases containing additives are lower than those of pure base grease. Addition of the lubricating additives dramatically improved the lubricating properties and led to decrease in the WSD and wear volume loss of the test ball. The WSD and wear volume loss of MoS_2 were 0.46 mm and 0.9×10^{-3} mm^3, respectively, and this material provided the most highly performance as the lubricating additive among some additives investigated.

Graphite, which was used as the starting material in this study, has also been well-known to the excellent additive of lubricant. The WSD and wear volume loss of graphite were 0.68 mm and 2.9×10^{-3}mm^3, respectively. It was found that the base grease with graphite did not represent better lubricating performance than that with MoS_2, but it largely improved in tribological quality relative to the base grease. EGO or C_{60} itself is decidedly inferior in lubricating performance as compared with the generally used lubricating additives such as MoS_2 and graphite as can be seen in Fig. 8. Similarly, the physically-mixed composite of EGO and C_{60}, which was prepared by grinding two species in a mortar, did not also show a good lubricating performance. However, the significant effect on friction improvement can be seen by the incorporating combination of C_{60} into EGO. The C_{60}/EGO composite prepared showed that a satisfactory in performance as the lubricating additive and the base grease with C_{60}/EGO composite after washed by toluene is particularly more efficient and provided better lubricating performance than that with other additives except MoS_2. It has been expected that C_{60} would be the ultimate lubricant, however, unfortunately it has been found that the addition of C_{60} between two surfaces is of little use. On the other hand, it has been reported by Averill et al. that intercalation of C_{60} into graphite caused the material to act as a fluid under pressure [38]. As described before, we showed that a C_{60} monolayer system confined by graphite layers exhibits superlubricity in our previous study. In the C_{60}/EGO composite synthesized in this study, the C_{60} does not construct a monolayer system but crystalline structure between the graphite plates, but there is an obviously difference in lubricating performance in the commercial product between C_{60}/EGO composite and the physically-mixed composite of graphite and C_{60}. In the C_{60}/EGO composite before washing with toluene, it is expected that excess C_{60}, which cannot be incorporated into the EGO interspaces, exist outside the EGO layers. It can be clearly seen in Fig. 8 that the C_{60}/EGO composite after washing improves the lubricating performance of the base grease than that before washing. This result suggests that a lubricating performance is strongly influenced by whether a C_{60} exists in the EGO interspaces or not and that the C_{60} on the surface of would reduce the lubricating performance. Further detailed investigations of the tribological behaviors and the lubrication mechanism of the C_{60}/EGO composite are now in progress.

Conclusions

We synthesized the C_{60}/EGO composite and investigated its lubricating properties in commercial grease. The XRD and SEM results confirmed that C_{60} in the C_{60}/EGO composite was incorporated into the EGO interspaces as the crystalline state.

The grease with C_{60}/EGO composite provides better lubricating performance than that with graphite. C_{60} and EGO was not effective in reducing friction in itself and the physically mixed composite of C_{60} and EGO did not also show a good lubricating performance as the additive similarly. The significant effect on tribological improvement can be seen by the incorporating of C_{60} into EGO. The C_{60}/EGO composite prepared in this study showed that a satisfactory in performance as the lubricating additive and the base grease with C_{60}/EGO composite after washed by toluene is particularly more efficient and provides better lubricating performance. This result suggests that C_{60} existed in the EGO interspaces plays an important role for the lubricating behaviors and that the C_{60} on the surface

would reduce the lubricating performance. In the C_{60}/EGO composite synthesized in this study, the C_{60} does not construct a monolayer system but crystalline structure between the graphite plates, but it is found that there is an obviously effect in lubricating performance in the commercial grease. The C_{60}/EGO composite found useful as antiware additive for lubricant.

Acknowledgements The authors would like to thank the staff in Chukyo Kasei Kogyo Co., Ltd for supporting triobological measurements and useful discussions.

References

1. Alexandre M, Dubois P (2000) Mater Sci Eng A 28:1
2. SinhaRay S, Okamoto M (2003) Prog Polym Sci 28:1539
3. Pan Y-X, Yu Z-Z, Ou Y-C, Hu G-H (2000) J Polym Sci B Polym Phys 38:1626
4. George JJ, Bhowmick AK (2008) J Mater Sci 43:702. doi: 10.1007/s10853-007-2193-6
5. Wang W-P, Pan C-Y (2004) Polymer 45:3987
6. Zheng G, Wu J, Wang W, Pan C (2004) Carbon 42:2839
7. Chen G, Lu J, Wu D (2005) J Mater Sci 40:5041. doi: 10.1007/s10853-005-1119-4
8. Song LN, Xiao M, Meng YZ (2006) Comp Sci Tech 66:2156
9. Zhao YF, Xiao M, Wang SJ, Ge XC, Meng YZ (2007) Comp Sci Tech 67:2528
10. Kojima Y, Usuki A, Kawasumi M, Okada A, Fukushima Y, Kurauchi T, Kamigaito O (1993) J Mater Res 8:1185
11. Yoshimoto S, Ohashi F, Ohnishi Y, Nonami T (2004) Synth Met 145:265
12. Yoshimoto S, Ohashi F, Kameyama T (2004) Macromol Rapid Commun 25:1687
13. Chung DDL (1987) J Mater Sci 22:4190. doi:10.1007/BF01132008
14. Lee S, Cho D, Drzal T (2005) J Mater Sci 40:231. doi:10.1007/s10853-005-5715-0
15. Kroto HW, Heath JR, O'Brien SC, Curl RF, Smalley RE (1985) Nature 318:162
16. Krätschmer W, Lamb LD, Fostiropoulos K, Huffman DR (1990) Nature 347:354
17. Wilson LJ, Cagle DW, Thrash TP, Kennel SJ, Mirzadeh S, Alford JM, Ehrhardt GJ (1999) Coord Chem Rev 190–192:199
18. Da Ros T, Prato M (1999) Chem Commun 8:663
19. Oberdörster E, Zhu S, Blickley TM, McClellan-Green P, Haasch ML (2006) Carbon 44:1112
20. Blau PJ, Haberlin CE (1992) Thin Solid Films 219:129
21. Taylor R, Avent AG, Dennis TJ, Hare JP, Kroto HW, Walton DRM, Holloway JH, Hope EG, Langley GJ (1992) Nature 355:27
22. Bharat Bhushan, Gupta BK, Van Cleef Garrett W, Cynthia Capp, Coe James V (1993) STLE Tribol Trans 36:573
23. Campbell SE, Luengo G, Srdanov VI, Wudl F, Israelachvili JN (1996) Nature 382:520
24. Gupta BK, Bharat Bhushan (1994) Lubr Eng 50:524
25. Mazin II, Rashkeev SN, Antropov VP, Jepsen O, Liechtenstein AI, Andersen OK (1992) Phys Rev B 45:5114
26. Scharff P (1998) Carbon 36:481
27. Saito S, Oshiyama A (1994) Phys Rev B 49:17413
28. Gupta V, Scharff P, Risch K, Romanus H, Müller R (2004) Solid State Commun 131:153
29. Kuc A, Zhechkov L, Patchkovskii S, Seifert G, Heine T (2007) Nano Lett 7:1
30. Lüthi R, Meyer E, Haefke H, Howald L, Gutmannsbauer W, Güntherodt H-J (1994) Science 266:1979
31. Li ZY (1999) Surf Sci 441:366
32. Okita S, Ishikawa M, Miura K (1999) Surf Sci 442:L959
33. Miura K, Kamiya S, Sasaki N (2003) Phys Rev Lett 90:055509/1-4
34. Miura K, Tsuda D, Sasaki N (2005) e-J Surf Sci Nanotech 3:21
35. Miura K, Tsuda D, Itamura N, Sasaki N (2007) Jpn J Appl Phys 46:5269
36. Hummers WS, Offeman RE (1958) J Am Chem Soc 80:1339
37. Heiney PA, Fischer JE, McGhie AR, Romanow WJ, Denenstein AM, McCauley JP, Smith AB, Cox DE (1991) Phys Rev Lett 66:2911
38. Averill BA, Sutto TE, Fabre J-M (1994) Mol Cryst Liq Cryst 244:77